J. Fluid Mech. (1965), *vol.* 23, *part* 1, *pp.* 99–111
Printed in Great Britain

Turbulent free convection in a vertical slot

By J. W. ELDER

Department of Applied Mathematics and
Theoretical Physics, Cambridge†

(Received 18 January 1965)

This paper is a continuation of the experimental study (Elder 1965), of free convection in a vertical slot, to unsteady and turbulent motion. The flow is specified by three dimensionless parameters: σ, the Prandtl number; $h = H/L$, the aspect ratio and

$$A = \gamma g \Delta T L^3/\kappa\nu,$$

the Rayleigh number. The present experiments are generally for $\sigma = 7$ (water), $h = 10$–30 and $A > 10^6$.

For A above about $8 \times 10^8 S/h^3$, travelling, wave-like motions grow up the hot wall of the slot and also down the cold wall. These waves grow most readily mid-way between the two ends. At higher values of the Rayleigh number when the wave amplitude is finite, the phase of successive wave fronts becomes increasingly random till near $A = 1{\cdot}0 \times 10^{10}/h^3$ an intense entrainment and mixing process commences between the wall region and the interior. The middle portion of the interior is then turbulent, the extent of the region growing further toward the ends as A increases.

Measurements of the mean temperature and the probability distribution of temperature fluctuations of the turbulent flow are reported. Except within the thin wall layers and distant from the ends, the interior has a mean temperature, uniform to within 0·1 %, superimposed on which is a nearly Gaussian fluctuation-field of variance of order $0{\cdot}01\Delta T$. A comparison is made with recent theories of turbulent convection; moderate agreement is found with the similarity ideas of Priestley (1959). The wall layer is seen as a marginally unstable sublayer.

1. Preliminary remarks

This paper considers experimental data for the unsteady and turbulent free convective flow in a vertical slot across which there is a uniform temperature difference. It is a continuation of a previous study (Elder 1965) which dealt with the corresponding steady motions.

Consider the motion of the fluid in a hollow rectangular prism of length L, breadth $\gg L$, and height H. Across the length let there be a uniform

† Present address: Institute of Geophysics and Planetary Physics, University of California, La Jolla, California.

temperature difference ΔT. The motion can be specified by three dimensionless parameters:

$$\left.\begin{aligned} \sigma &\equiv S^2 = \nu/\kappa, && \text{the Prandtl number;} \\ A &= \gamma g \Delta T L^3/\kappa\nu, && \text{the Rayleigh number;} \\ h &= H/L, && \text{the aspect ratio.}\dagger \end{aligned}\right\} \tag{1}$$

The present experiments were mainly with water ($\sigma \doteqdot 7$); the aspect ratio was in the range 10–30, while the value of A was $A > 10^6$.

The first extensive measurements for this problem of unsteady flow, the heat-transfer measurements of Mull & Reiher, have been discussed by Jakob (1949)

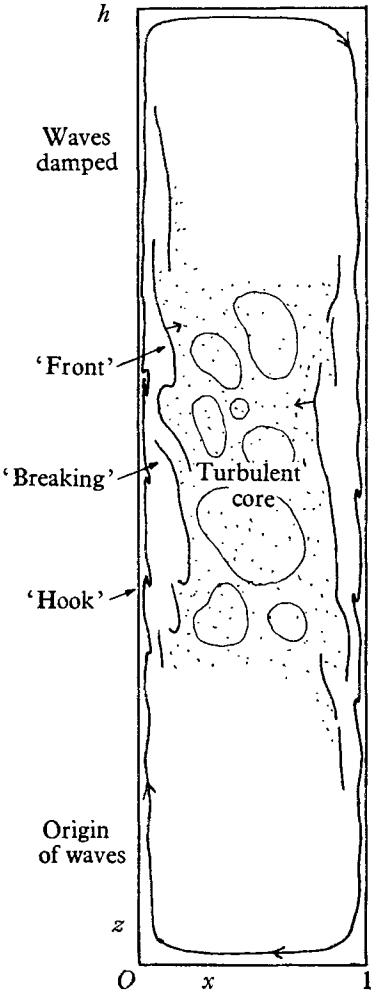

FIGURE 1. Schematic diagram of the slot and the flow régimes, showing the growth of the wall waves, the 'fronts', and the turbulent core. Compare figures 2, 3 and 6. (Note: in all diagrams the hot wall is on the left-hand side.)

† The notation follows Elder (1965). Note that L, ΔT are used as units of length and temperature. The dimensionless temperature is θ. Dimensional quantities are indicated by an asterisk (*).

and by Batchelor (1954). Recently Mordchelles-Regnier & Kaplan (1963) have obtained measurements and visualizations up to Rayleigh numbers of order 10^{12}. The flow near the walls is very similar to that in the boundary layer of an isolated vertical plate ($h \ll 1$) for which Eckert, Soehngen & Schneider (1955) and Szewczyk (1962) have studied the flow by visualization techniques.

Our main interest here is in the recent ideas of free convective turbulence of Malkus (1963) and Priestley (1959). Both these theories purport to apply to a flow in which: (i) the motion is fully turbulent, and (ii) the mean heat flux is independent of position. Hitherto, experimental investigation of these two theories has been largely restricted to the case in which the mean heat flux is vertical (e.g. Townsend 1959). But the flow in a vertical slot, at sufficiently high Rayleigh numbers, also satisfies the two requirements of the theories. The advantage of the vertical slot is that the onset of fully developed turbulence is readily apparent.

Since it is necessary to be assured that the flow is fully turbulent some investigation of the onset of turbulence is required. These experiments are described in § 2. The measurements of the fully turbulent flow are described in § 3 and discussed in § 4.

Figure 1 schematically represents the possible flow régimes. Up to a value of A of about 10^6 the motion in the slot is steady. At higher values of A unsteady motions appear; these originate in the wall regions and are initially travelling wave-like motions. Increasing A further leads to breakdown of the regular wave motion into an intense mixing region which first appears near $z = \frac{1}{2}h$, the overlapping region between the two trains of 'breaking' waves, one travelling up the hot wall, one travelling down the cold wall, inducing a turbulent zone in the central portion of the interior. The vertical extent of this turbulent core increases with A.

2. The approach to turbulence

The wall waves

Up to a value of A of order 10^6 there are two possible steady motions in the slot, heretofore called the primary and secondary flows (Elder 1965). Near $A = 10^7$ the secondary flows are observed to be somewhat unsteady; frequently isolated quasi-steady single cells of the secondary type are seen. This phenomenon has not been studied in any detail because at slightly higher Rayleigh numbers we observe the appearance of a further instability of the primary flow, the wall waves. These are produced by an instability of the wall region and are similar to those found on an isolated vertical plate. When the waves appear they gradually disrupt the steady cellular pattern in the interior, and although it is possible to have secondary flows co-existing with the wall waves, in general the steady cellular motions are completely disrupted.

Figure 2 (plate 1) shows a visualization of the wall waves obtained by injecting dye into the slot interior. These photographs are similar to visualizations obtained by, e.g., Eckert *et al.* (1955), Szewczyk (1962) and Mordchelles-Regnier & Kaplan (1963). Figure 2 (*a*) shows a view of the entire flow space,

while figure 2 (*b*) is a close-up of the middle of the hot wall. On the hot wall the waves originate near $z^* = 13$ cm (this cannot be clearly seen on the photograph shown), grow rapidly near $z^* = 27$ cm, and appear to be damped above $z^* = 36$ cm although wave-fronts can still be seen up to $z^* = 51$ cm. It was generally observed that the amplitude of the waves near the critical Rayleigh number was a maximum at $z = \frac{1}{2}h$. The waves, when they reach the form seen in figure 2 (*b*), travel at a speed close to that of the maximum wall-layer velocity.

Experimental values for the onset of the boundary-layer waves

Measurements with apparatus I, $L = 2, 5, 6$ cm and $H = 55$ cm, gave the onset of boundary-layer waves at

$$(Az^3)_c = 3 \times 10^8 \pm 30\ \% \quad (\sigma = 7). \tag{2}$$

The bulk of the experiments were performed with water, but in the course of the low A studies with silicon oil in apparatus II, waves were found for $\Delta T \geqslant 50\ ^\circ$C for which

$$(Az^3)_c = 3 \times 10^9 \pm 30\ \% \quad (\sigma = 10^3). \tag{3}$$

Unfortunately, little attention was given to this at the time, but it would appear that there is a Prandtl-number dependence. Assuming that $(Az^3)_c \propto S^p$ requires $p \sim 1 \pm 0{\cdot}25$. Whence (2) and (3) can be combined into a single very crude result

$$(Az^3)_c = 1{\cdot}0 \times 10^8 S \pm 30\ \%. \tag{4}$$

Noting that the maximum amplification of the waves is at $z = \frac{1}{2}h$, equation (4) gives a least value of A of

$$A_c = 8 \times 10^8 S/h^3. \tag{5}$$

The vertical wavelength λ of the wall wave has been determined by inspection of thirteen photographs (VS 10: 1–13) of flows not greatly above critical. Using $\delta_\odot$ as the distance to the velocity maximum, so that defining $n = \delta_\odot/\lambda$, the experimental values give $n = 0{\cdot}18 \pm 0{\cdot}03$. A more accurate determination of n would be very difficult.

The measurements here may be compared to those made with an isolated vertical plate. Tritton (1963) has remarked on the large range of reported values of the critical Rayleigh number. Of these the estimate given by Eckert *et al.* (1955) is in closest accord with (4). They find that in air

$$(Az^3)_c = 3 \times 10^8 = 3{\cdot}5 \times 10^8 S,$$

differing from the present estimate by a factor of 3·5. On the other hand, Mordchelles-Regnier & Kaplan (1963) give in their table 1 values of

$$(Az^3)_c = 2\text{–}30 \times 10^8.$$

Such a range of values suggests the existence of a further parameter in their system. Szewczyk (1962) states that $(Az^3)_c = 5 \times 10^9$ for water, but it is very doubtful if this value corresponds to the first appearance of the wall waves. Lacking evidence to the contrary it can only be assumed that Szewezyk has not identified the origin of the wall waves correctly.

Kurtz & Crandall (1962) have investigated theoretically the condition for the appearance of the wall waves on a single vertical plate on the assumption that buoyancy forces are negligible. They obtain for air a critical Reynolds number, based on the maximum velocity and the wall-layer thickness, of 161. They

observe that this prediction differs considerably from the value of 630 found by Eckert & Soehnghen (1951). The prediction implies that $(Az^3)_c \sim 10^8\sigma^4$ (using the solution of Squires). This cannot be reconciled with result (4). In spite of the large variability of the measurements, the data suggest that buoyancy forces play a role in the generation of the wall waves.

Gershuni (1955) has given some solutions of the stability problem with buoyancy retained. Unfortunately the steady temperature and velocity profiles he uses refer only to those found at small Rayleigh numbers ($A < 10^4$). In these circumstances not even steady secondary flows are possible (Elder 1965). However, a crude result applicable to the wall layer can be obtained by considering the region from $x = 0$–$\frac{1}{2}$ in Gershuni's calculation as the wall layer. Hence defining δ_s such that the Nusselt number $N = \frac{1}{2}\delta_s$ (whence in Gershuni's calculation $\delta_s = \frac{1}{2}$) we have

$$A_s \equiv \gamma g(\tfrac{1}{2}\Delta T)\,\delta_s^3/\kappa\nu \sim 800, \tag{6}$$

using Gershuni's result $A_c \sim 1{\cdot}2 \times 10^4$. This may be compared to the very crude experimental values of A_s of about 400 for water and 1600 for oil. At least these figures agree in order of magnitude. But clearly more careful experimental and theoretical work is necessary.

Finite amplitude waves

Observations with suspended aluminium powder reveal that initially the waves are detectable as slight oscillations of the stream lines. But as they grow in amplitude the outer portion of the wave curls over and, relative to the head of the wave front, is left behind. These hook-like structures are clearly seen in figure 2 (*b*), (plate 1).

Mordchelles-Regnier & Kaplan (1963) report critical values of the parameters for the wall waves. These values refer to the first appearance of the wave profile as being as shown in figure 2 (*b*), i.e. with a hook-shape. The data of their table 2 is rather difficult to correlate satisfactorily; especially so is their run at large h (25–250) for which values of A range from 2×10^5 to $1{\cdot}5 \times 10^3$. I cannot reconcile these small values of A with any of this work. Lacking evidence to the contrary I presume that they are transient effects; that is, the flow had not reached a steady state. Apart from this, their data gives

$$\beta A = 10^7 \pm 50\,\%, \tag{7}$$

where β is the vertical temperature gradient in the interior. Though this correlation is poor, it does suggest that the vertical temperature gradient plays a strong role in the growth of the wave amplitude. For $\beta > 0$, as the wave rises in the layer, a point can be reached at which a portion of the wave front is at a lower temperature than the interior. This portion will be the outer part of the wave-front distant from the temperature source of the wall. It will thereby be decelerated and fall behind.

The onset of turbulence

Initially the wall waves are small in amplitude and the wave train is regular. However, at higher values of A when the wave amplitude is finite the waves

become increasingly irregular. There is a progressive change of amplitude and phase as the wave progresses—we now have a dispersive wave. Near

$$A_c h^3 = 1{\cdot}0 \times 10^{10}$$

($h = 12$ for water) the wave train 'breaks' and an intense interaction commences between the wall region and the interior. An intense mixing region, existing in the wall layer, entrains fluid from the interior and ejects it out again. The violence of this interaction is comparable to that of turbulent transition near the wall of a body placed in a flowing stream.

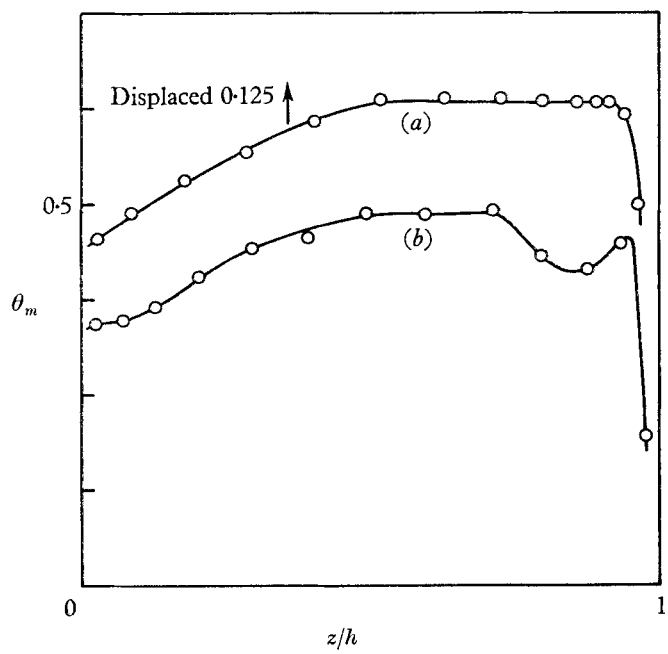

FIGURE 4. Centre-line temperature, $\theta_m(z/h)$; $L = 5{\cdot}0$ cm; $H = 56{\cdot}8$ cm. (*a*) $\Delta T = 42{\cdot}2$ °C, $A = 2{\cdot}3 \times 10^8$. (*b*) $\Delta T = 20{\cdot}5$ °C, $A = 1{\cdot}0 \times 10^8$.

Numerous estimates of the Rayleigh number at which the wall layer is turbulent can be found in the literature. Tritton (1963) finds a fair measure of agreement with these and his own estimate, $(Az^3)_c = 1{\cdot}0 \times 10^9 \pm 30\,\%$ for a vertical plate. Breaking first occurs near $z = \frac{1}{2}h$ for which $A_c(\frac{1}{2}h)^3 = 1{\cdot}3 \times 10^9$, a value similar to that given by Tritton. We may conclude that the occurrence of a turbulent wall-layer in the slot is independent of h and occurs in a similar manner to that on an isolated vertical plate.

Figure 3 (plate 2) is a streak photograph of the 'breaking' region. It reveals 'fronts' which move obliquely outward from the wall region; these separate regions of hot fluid near the wall from the relatively cooler fluid of the interior. The width of these 'fronts' is quite small compared to the boundary-layer thickness.

The mixing regions isolate the interior from the stabilizing influence of the walls, while providing random finite-amplitude disturbances to the interior.

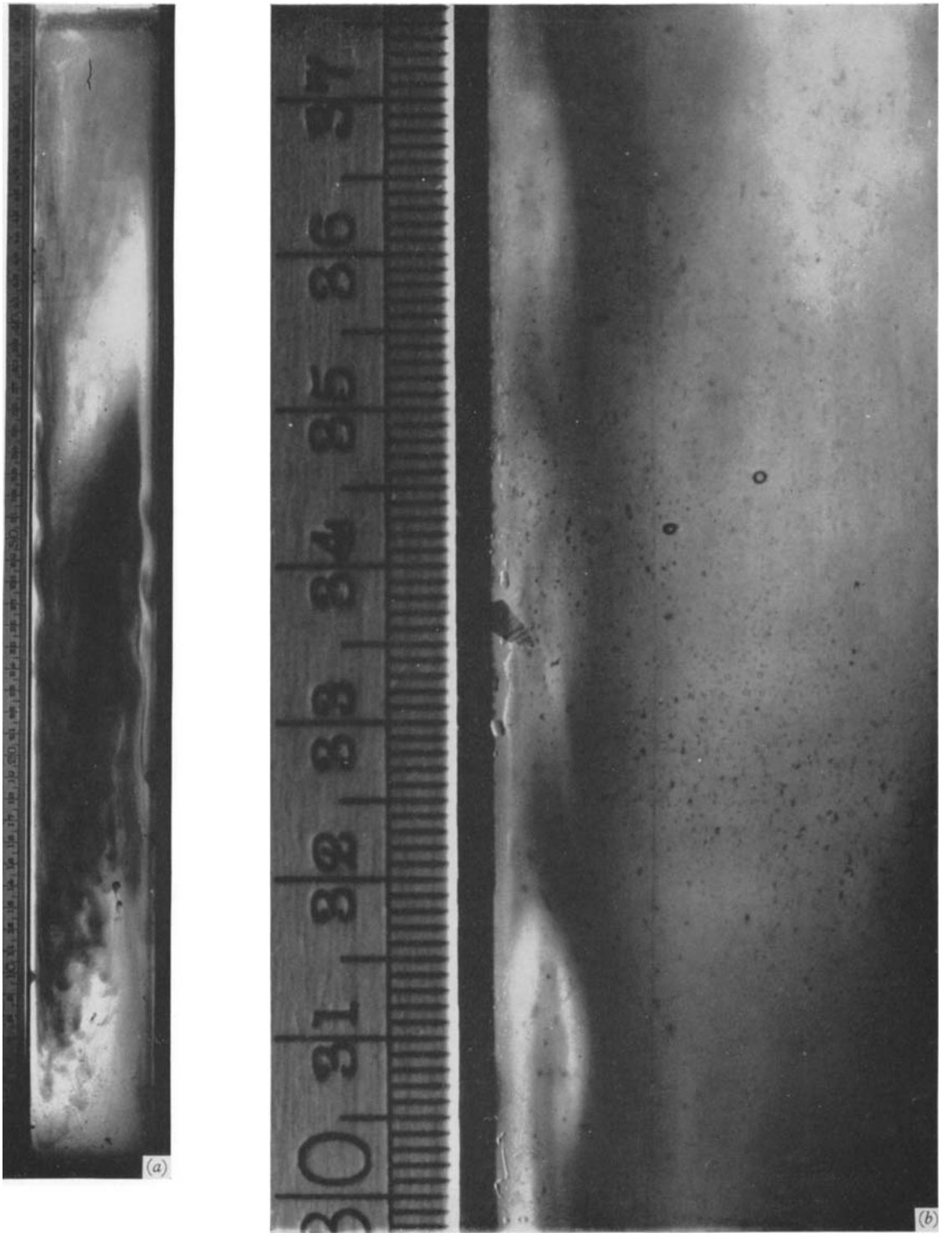

FIGURE 2. Photograph of the wall waves obtained with dye injection; $A = 2{\cdot}2 \times 10^7$ ($L = 6{\cdot}0$ cm, $H = 54{\cdot}8$ cm, $T = 5{\cdot}1$ °C). (*a*) Full view. (*b*) Detail showing 3 wave-fronts (VS 10: 6, 7).

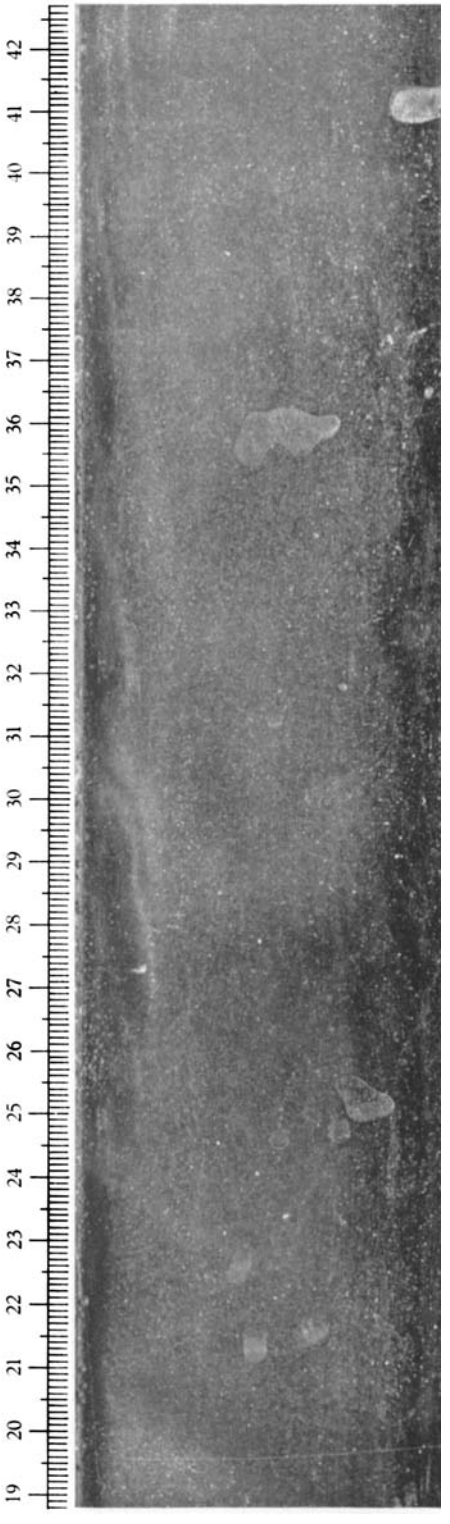

FIGURE 3. Photograph of the wave entrainment zone; $A = 1{\cdot}3 \times 10^8$ ($L = 6{\cdot}0$ cm, $H = 57{\cdot}9$ cm, $\Delta T = 16{\cdot}8$ °C; VS 10: 19), $\frac{1}{5}$ sec exposure.

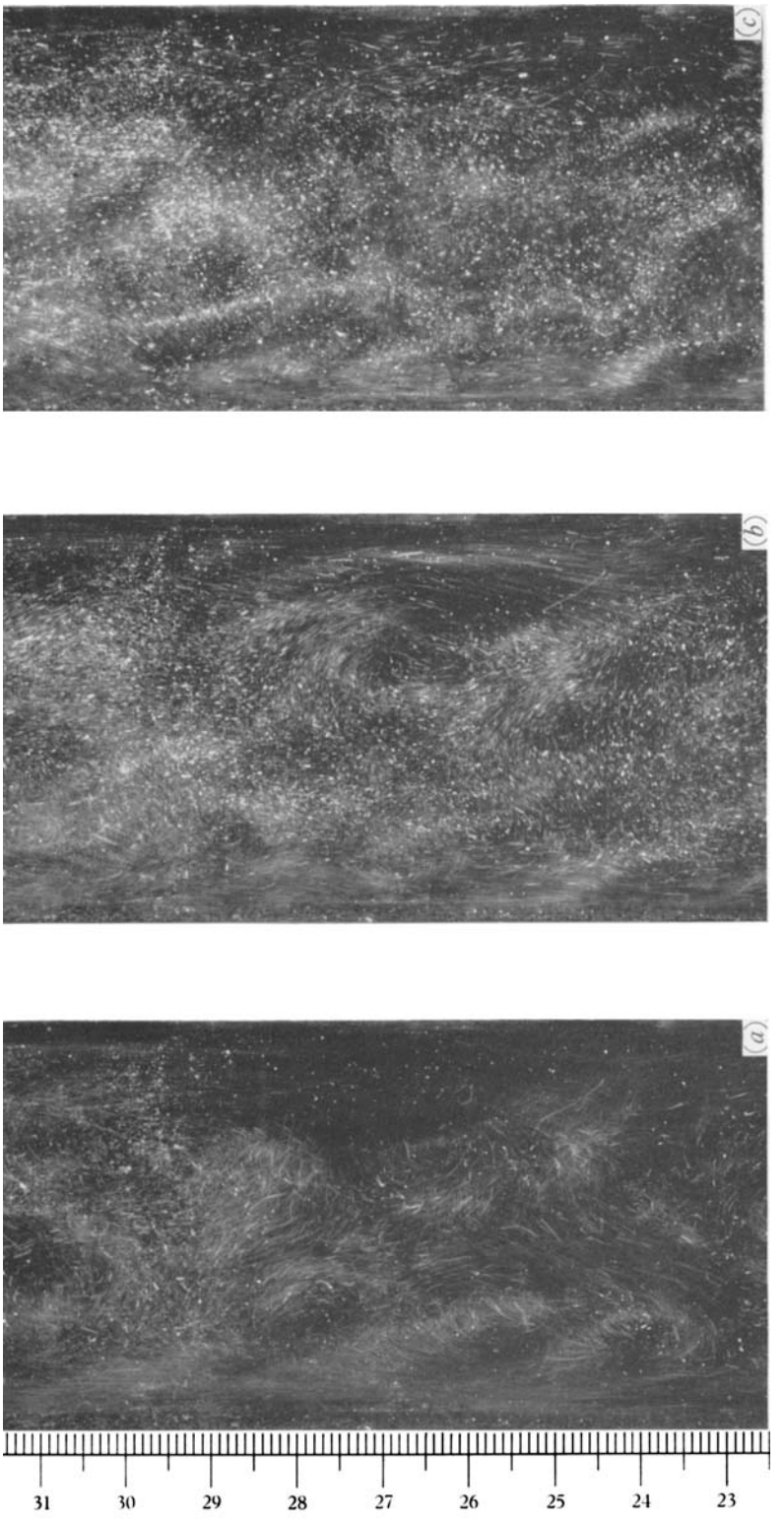

FIGURE 6. Photographs of the turbulent region; parameters as in figure 4(*a*). Exposure time: (*a*) 1 sec, (*b*) $\frac{1}{5}$ sec, (*c*) $\frac{1}{25}$ sec (VS 11 : 8, 6, 4).

Marked changes in the mean properties of the interior result. Hitherto the interior has closely approximated $U = 0$, $W = W(x)$, $\theta = \theta_{m0} + \beta z + \Theta(x)$ both for the steady flows (Elder 1965) and while the wall waves were present. Figure 4 shows the effect of 'breaking' on θ_m, the centre-line temperature, for two values

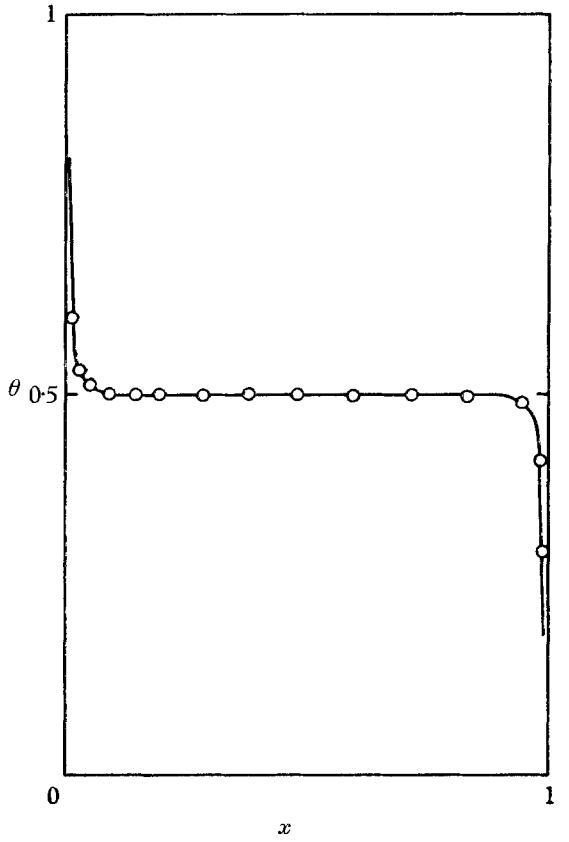

FIGURE 5. Temperature profile, $\theta(x)$ at $z = \frac{1}{2}h$; parameters as in figure 4(*a*).

of ΔT in the 'breaking' range. In the lower portion of the slot a strong adverse vertical gradient still exists with $\beta h = 0{\cdot}3$–$0{\cdot}4$. Near $z/h = 1$ the temperature distribution is dominated by the heat lost through the upper free surface. But between these two regions there now exists a region of zero vertical temperature gradient. This region grows with ΔT and indicates the zone of overlap of the mixing regions on the two walls.

Figure 5 shows a temperature profile measured between the mixing regions. It reveals, as before, wall regions of large horizontal temperature gradients, but outside these there is no longer a horizontal temperature gradient.

Thus within the interior, between the mixing regions, there exists a uniform mean temperature field. The occurrence of this is so marked that in these experiments a uniform temperature zone was taken as the indicator of the presence of turbulence in the interior.

These results were confirmed by measurements made with apparatus III, a uniformly heated cylinder surrounded by a fluid annulus. With this arrange-

ment the temperature difference between the heated wall and the cooled wall increased with z. The temperature difference was measured with a string of thermocouples imbedded in the walls. From 3 runs at $A_h = 0{\cdot}43, 1{\cdot}30, 2{\cdot}80 \times 10^9$ in water it was found that the local Nusselt number N' decreased up the slot like $z^{-\frac{1}{4}}$ till $z/\delta \sim 170$ beyond which N' remained constant (i.e. ΔT was constant). These results are similar to those found by Griffiths & Davis (discussed by Jakob 1949, § 25–2). By looking at a vertical slit of light through the apparatus it was observed that wall waves appeared in all three runs near $z/\delta \sim 120$ and were strongly established at $z/\delta \sim 170$.

3. The fully-turbulent flow

The assertion that the region of uniform temperature, revealed by the data of figures 4, 5, is turbulent, is confirmed by visualizing the flow by means of suspended aluminium powder. Figure 6 (plate 3) shows three such photographs covering exposure times from $\frac{1}{25}$ to 1 sec; i.e. a velocity scale range of 25:1. Figure 6 (*c*) with the shortest exposure time reveals only the strongest motions in the interior; the bulk of the motion occurs near the walls, where there is a strong mean vertical component. Several 'fronts' are seen (especially near the hot wall in this photograph). The interior shows a quasi-cellular structure. Figure 6 (*b*) reveals strong eddying motions of length-scale comparable with L. Figure 6 (*a*) emphasizes the motion in the interior. There is no evidence of any mean motion in the interior. Thus the turbulent interior is a region of uniform mean temperature and zero mean velocity.

Experimental procedure

Because of the importance of the mean temperature field in recent theories the greatest care was taken to measure the mean temperature profile. The thermocouple e.m.f. (measuring the temperature difference between the probe and a reference junction in the cold wall) was taken to a potentiometer giving an accurately known backing voltage, the output of which fed a chopper amplifier of gain up to 10^5 and full-scale rise time 0·4 sec with noise referred to input of about 0·1 microvolt, negligible drift (less than 0·1 microvolt during a run) and linearity of order 0·1 %. The amplifier output then fed either an electronic integrator or a chart recorder, or both. The linearity of the integrator was of order 0·1 %. Most of the runs were with $\Delta T \sim 50\,^\circ\mathrm{C}$; the thermal e.m.f. is of order $40\,\mu\mathrm{V}/^\circ\mathrm{C}$, so that the possible accuracy of the system for a measurement to the nearest microvolt is $\pm 0{\cdot}025$ % (the backing voltage could not be set more accurately). The most troublesome feature of the experiment was to maintain ΔT sufficiently constant. During the better runs changes in ΔT were less than 0·01 °C so that measurement to the nearest microvolt ($\pm 0{\cdot}01\,^\circ\mathrm{C}$) was about the limit of the system. At this level no significant error was introduced by the amplifier or the integrator.

It has already been pointed out by Townsend (1959) that the temperature fluctuations of thermal turbulence cover a wide spectrum and that to find a mean value very long integration times are needed. On the other hand, the longer the

period of integration the greater the drift in ΔT. One needs to measure θ at a number of points, and it is the drift in the total time that is relevant. Nevertheless, there was little difference in the results (viz. $\pm 1\,\mu$V) for integration times of 100–1000 sec; the results quoted here are for 300 sec integration. It is worth remarking that the strongly intermittent nature of the fluctuations makes reliable measurements by 'hand', e.g. watching the needle of a galvanometer of long period, almost impossible.

Experimental data

The best data run is shown in figure 7 by plotting $(\theta - \theta_m)$ as a function of x for measurements near the hot wall. Other measurements showed no significant difference in the form of this function as measured near either $x = 0$ or $x = 1$.

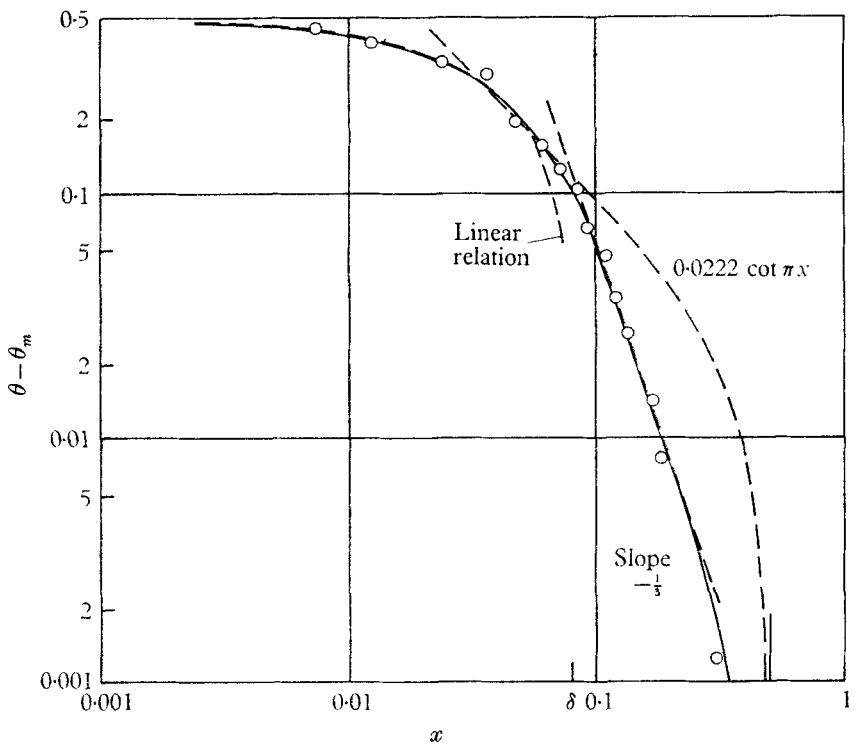

FIGURE 7. Logarithmic plot of $\theta(x) - \theta_m$; $A = 4{\cdot}1 \times 10^7$; apparatus II: $z = \frac{1}{2}h$.

Near the wall there is a uniform mean temperature gradient corresponding to $(\theta - \theta_m) = \text{const.}\ (\delta - x)$—this region is indicated by the phrase 'linear relation'. This is the sublayer. The region $0{\cdot}25 < x < 0{\cdot}75$ is that of the fully turbulent core; here the mean temperature is uniform to $\pm 0{\cdot}001\Delta T$. Between these two regions is the mixing region, where the mean temperature fairs smoothly from a constant to a linear relation over the range $0{\cdot}05 < x < 0{\cdot}25$. A line of slope $-\frac{1}{3}$ has been drawn on the figure and will be referred to below.

By feeding the output of the amplifier into a chart recorder (1 sec time to full scale) and evaluating the ordinate distribution, the probability distribution

of temperature $P(\theta)$ could be estimated. (Note that the frequency response of the system was limited to frequencies below about 5 c/s.) $P(\theta)$ is normalized such that $\int_0^1 P(\theta)\,d\theta = 1$. Figure 8 shows several such distributions. Greater

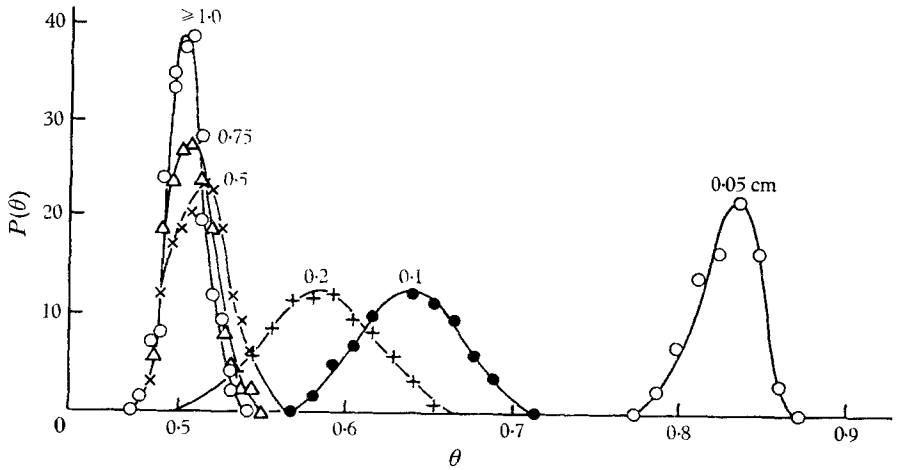

FIGURE 8. Temperature probability distribution, $P(\theta)$ at $A = 4{\cdot}1 \times 10^7$ for indicated values of x^*; apparatus II, $L = 4{\cdot}08$ cm.

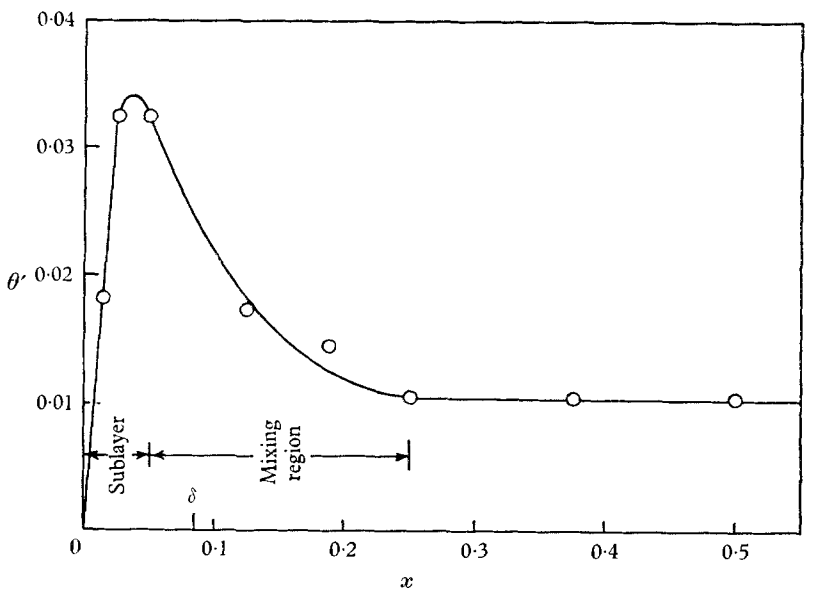

FIGURE 9. R.m.s. temperature fluctuation $\theta'(x)$, corresponding to the data of figures 7 and 8.

intensity of the temperature fluctuations is indicated by the greater width of a distribution and correspondingly smaller values of P. This is more clearly seen in figure 9 which shows the corresponding root-mean-square temperature fluctuations. Thus the fluctuations are strongest in the sublayer and the mixing region.

Notice further that both in the core and in the middle of the mixing region the probability distributions are symmetrical. This is not the case near the wall or in the region between the interior and the mixing region. The distributions here are skew. Note also that temperature fluctuations as large as $0{\cdot}1\Delta T$ are rather common. This is about as large as the entire temperature change between the two sublayers. In other words, variations in the mean temperature are generally small compared to fluctuations about the mean temperature.

4. Discussion of the turbulence data

Close inspection of the ideas of thermal turbulence proposed by Priestley (1959) and Malkus (1963) shows that the angles between the directions of gravity and the mean heat flux are not invoked except in the sublayers. Their ideas can therefore be used here.

If there is a region near $x = 0$ (or $x = 1$) where the transfer of energy and momentum is dominated by turbulent processes rather than by molecular diffusion, Priestley (1959) has shown that the heat flux

$$F = a\rho(c[\theta^* - \theta_m^*])^{\frac{3}{2}}(\gamma g x^*/c)^{\frac{1}{2}} \qquad (a = \text{const.}), \tag{8}$$

where c is the specific heat. This relation can be expected to be valid only in the region of intense mixing. It will not be valid in the sublayer where molecular processes dominate, nor in the interior where the direct influence of the walls is negligible. Figure 8 shows a region of slope $-\frac{1}{3}$, as required by (8), covering at least the range $0{\cdot}01 < (\theta - \theta_m) < 0{\cdot}1$, with $a \doteqdot 0{\cdot}275$. Visual observation, e.g. as in figure 6, shows that this is certainly the region of most vigorous mixing.

The theory of Malkus (1963) requires

$$\theta - \theta_m = (A_0/A)^{\frac{1}{3}} \cot \pi x, \quad A_0 = \text{const.} \tag{9}$$

A curve of the form (9) can be fitted to the experimental data by noting that as $x \to \frac{1}{2}$, $\theta \to \theta_m$. There remains the coefficient $(A_0/A)^{\frac{1}{3}}$, which can be varied to provide the best fit; this can best be done by matching in the region near $x = 0$, where $\cot \pi x \propto x^{-1}$ (relation (9) does not purport to be valid in the sublayer). The fit shown corresponds to $A_0 \doteqdot 450$. Otherwise, the fit is disappointing in the mixing region.

Malkus evaluates A_0 by invoking marginal stability on the mean temperature profile. In his calculations the contribution to A_0 arises largely in the sublayer, where the mean profile changes most rapidly. An independent check on this idea can be obtained from a consideration of the experimental values of heat transfer.

The Nusselt number N has been determined by several workers but most extensively by Mull & Reiher (Jakob 1949) who find

$$N/A^{\frac{1}{4}} \sim \text{const.}, \quad A \lesssim 10^6, \tag{10}$$

$$N/A^{\frac{1}{3}} \sim C(\sigma), \quad A \gg 10^6. \tag{11}$$

It should be noted that both relations are asymptotic, i.e. with h fixed but $H \to \infty$. Further, when $A > 10^6$ part of the wall layer will transfer heat as in (10), part as in (11), in which case $N(A)$ will differ from both (10) and (11). The value of $C(\sigma)$ is rather uncertain, but from Mull & Reiher's data, assuming C inde-

pendent of h and σ, we find $C = 0{\cdot}053 \pm 6\,\%$. The relation (11) can be used to define a Rayleigh number for the wall region or sublayer. Thus writing $N = \frac{1}{2}\delta_s$, δ_s is a measure of the thickness of the sublayer. Across this region there is an effective temperature drop $\frac{1}{2}\Delta T$. Hence

$$A_s \equiv \tfrac{1}{2}A\delta_s^3 = (\tfrac{1}{16}C)^3 = 400 \pm 20\,\%, \tag{12}$$

a value close to $A_0 = 450$ obtained experimentally from (9). It is also of the same order as the estimate in (6) of the wall-layer critical Rayleigh number. Thus (12) could be interpreted as the condition relating to the marginal instability of the sublayer.

The motion at large Rayleigh numbers can thus be interpreted in terms of three regions: sublayer, mixing region and interior. Thermal energy transferred by thermal conduction accumulates in the sublayer where there is a strong mean motion superimposed on which are wave-like structures. It has been suggested that the sublayer is controlled by a local sublayer Rayleigh number, that is, through a balance of buoyancy and viscous forces. The layer is marginally stable and frequently elements are rapidly ejected from the layer as oblique fronts. Presumably this arises through a rapidly occurring imbalance between buoyancy and viscous forces leading to large local accelerations. The mechanism of this instability process is not understood. As the element accelerates out of the sublayer it will locally reduce the thermal energy of the sublayer. The elements move sufficiently rapidly out of the sublayer for molecular processes to be negligible in the mixing region. The interior is continually stirred by random buoyant elements of finite energy.

The evidence of figure 7 should not be regarded as conclusive. It does, however, support the 'similarity' hypothesis rather better than that of Malkus. This does not discount the Malkus theory, but it suggests that any such theory must incorporate a zone outside the conduction region where diffusive effects are small in the mean.

I would like to thank: W. G. Pye, Cambridge, for supplying the chopper amplifier and the integrator; the Cambridge Instrument Company for supplying the chart recorder; and Mr W. G. Garner who built most of the apparatus. This work was supported by the British Admiralty. The manuscript was written while I was supported from National Science Foundation Grant GP-2414 and Office of Naval Research Contract Nonr-2216.

REFERENCES

Batchelor, G. K. 1954 *Quart. Appl. Math.* **12**, 209.

Eckert, E. R. G. & Soehnghen, E. 1951 Proceedings of the General Discussion on Heat Transfer. London. *Inst. Mech. Engrs*, p. 321.

Eckert, E. R. G., Soehngen, E. & Schneider, P. J. 1955 *50 Jahre Grenzschichtforschung*, p. 407. Berlin: Vieweg & Sohn.

Elder, J. W. 1965 *J. Fluid Mech.* **23**, 77.

Gershuni, G. Z. 1955 *Zh. tekh. Fiz.* **25**, 351.

Jakob, M. 1949 *Heat Transfer*. New York: Wiley.

Kurtz, E. F. & Crandall, S. H. 1962 *J. Math. Phys.* **41**, 264.

MALKUS, W. V. R. 1963 *Theory and Fundamental Research in Heat Transfer* (ed. J. A. Clarke), p. 203. London: Macmillan.

MORDCHELLES-REGNIER, G. & KAPLAN, C. 1963 *Proc. Int. Heat & Mass Transf. Conf.* p. 94.

PRIESTLEY, C. H. B. 1959 *Turbulent Transfer in the Lower Atmosphere.* Chicago: University Press.

SZEWCZYK, A. A. 1962 *Int. J. Heat & Mass Transf.* **5**, 903.

TOWNSEND, A. A. 1959 *J. Fluid Mech.* **5**, 209.

TRITTON, D. J. 1963 *J. Fluid Mech.* **16**, 269, 417.